

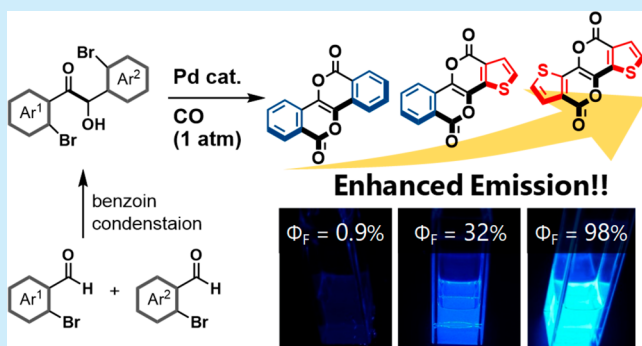
Palladium-Catalyzed Double Carbonylative Cyclization of Benzoin: Synthesis and Photoluminescence of Bis-Ester-Bridged Stilbenes

Yosuke Tani*¹ and Takuji Ogawa*

Department of Chemistry, Graduate School of Science, Osaka University, Machikaneyama 1-1, Toyonaka, Osaka 560-0043, Japan

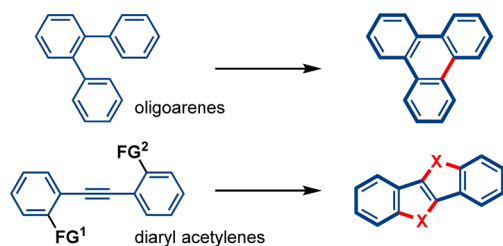
S Supporting Information

ABSTRACT: A palladium-catalyzed double carbonylative cyclization of benzoin has been developed, which realizes the synthesis of bis-ester-bridged stilbenes just in two steps from aldehydes. Thus, the obtained fully fused tetracyclic π -systems have a pyrano[3,2-*b*]pyran-2,6-dione (PPD) core on their center, showing two reversible reductions at low potentials. In addition, their photoluminescence properties are strikingly affected by the aromatic rings fused to the PPD core; bis-*thieno*-fused PPDs are found to be excellent fluorophores with quantum yields up to 0.98.



Polycyclic fused π -conjugated systems such as bridged stilbenes, triphenylenes, and acenes are a privileged motif in optical and electronic materials, including organic light-emitting diodes and organic photovoltaics.¹ Therefore, efficient synthetic strategies for such fused skeletons are of great interest.² Many of the established routes construct them from preorganized, nonfused π -systems (Figure 1a), e.g. from oligoarenes by Scholl reaction or direct arylation,³ or from

a) Pre-organized, non-fused π -systems as precursors



b) Benzoin as a key precursor (concept of this work)

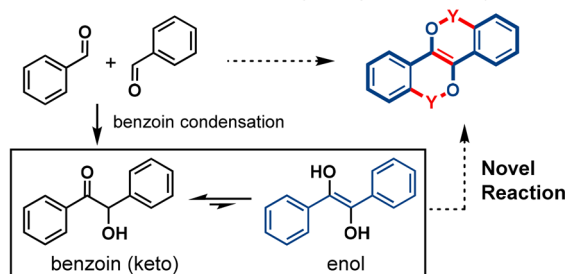


Figure 1. Synthetic strategy toward polycyclic fused π -systems utilizing (a) preorganized π -systems and (b) benzoin as an easily available, latent π -system (This work). FG = functional group.

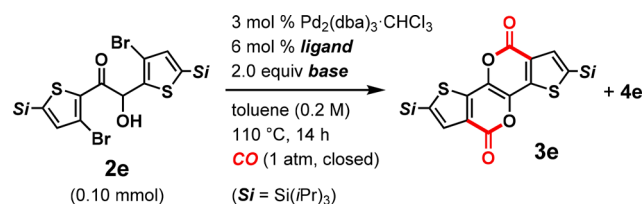
functionalized diaryl acetylenes into bridged stilbenes.⁴ In this context, benzoin can be a promising precursor for fused π -systems, since they are available directly from aldehydes by benzoin condensation and have a stilbene skeleton in the enol form (Figure 1b). The development of a suitable transformation of benzoin will expand the chemistry of bridged stilbenes that are otherwise difficult to access. In particular, bis-ester-bridged stilbenes (Y is C=O in Figure 1b) are attractive because the ester group is electron-withdrawing, chemically convertible, and redox active, and it composes a weakly aromatic 2-pyrone substructure.^{5,6} Interestingly, they are also found in some natural products.⁷ Nonetheless, the synthesis and properties of bis-ester-bridged stilbenes are virtually unexplored.⁸

We envisioned that Pd-catalyzed carbonylation chemistry⁹ would offer a powerful solution for the conversion of benzoin into bis-ester-bridged stilbenes. In particular, carbonylative cyclization has been utilized in the synthesis of heterocycles,¹⁰ although the construction of multiple rings is rarely achieved.¹¹ Herein, we have developed a palladium-catalyzed double carbonylative cyclization of benzoin, which affords bis-ester-bridged stilbenes having a pyrano[3,2-*b*]pyran-2,6-dione (PPD) core on its center. The reaction reveals a stilbene skeleton, fixes the planar π -system, and installs electron-withdrawing functionality at one time, thus providing them with unique electronic and photophysical properties.

We began by benzoin condensation of 2-bromoarylaldehydes 1a–1e, which are readily available by several approaches (Scheme S1 in the Supporting Information (SI)).¹² After the corresponding benzoin 2a–2e were successfully synthesized, double carbonylative cyclization of 2e was examined under various conditions (Table 1). The reaction mainly produced

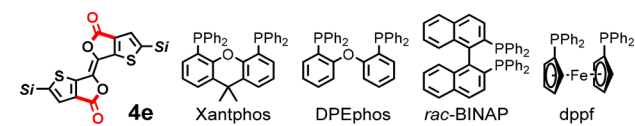
Received: October 4, 2018

Table 1. Pd-Catalyzed Double Carbonylative Cyclization of 2e



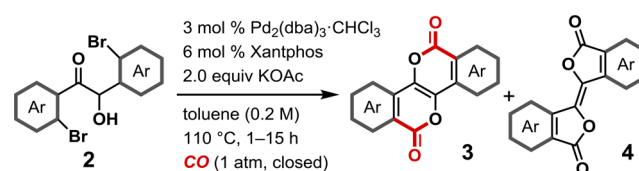
entry	ligand	base	yield (%) ^a	3e/4e ^b
1	Xantphos	Cs ₂ CO ₃	42	>95/5
2	Xantphos	CsOAc	88	85/15
3	Xantphos	KOAc	95	87/13
4	Xantphos	NaOAc	49	>95/5
5	DPEphos	KOAc	65	60/40
6 ^c	dppf	KOAc	52	42/58
7	<i>rac</i> -BINAP	KOAc	20	25/75
8 ^d	Xantphos	KOAc	76	88/12
9 ^d	Xantphos	KOAc ^e	92	85/15

^aCombined yields of 3e and 4e determined by ¹H NMR using 1,3,5-trimethoxybenzene as an internal standard. ^bDetermined by ¹H NMR. ^cPdCl₂(dppf) (6 mol %) was used as the catalyst. ^dPdCl₂(PhCN)₂ (6 mol %) was used instead of Pd₂(dba)₃·CHCl₃. ^eKOAc (3.0 equiv) was used.



fully fused target 3e and its structural isomer 4e, and was quantitatively evaluated by ¹H NMR using an internal standard. First, we tested the effect of a base by using Pd₂(dba)₃·CHCl₃ as a catalyst precursor and Xantphos as a ligand^{9b} under 1 atm of carbon monoxide (CO) in toluene at 110 °C (entries 1–4). When we used Cs₂CO₃, 3e was obtained in 42% yield (entry 1), which was the highest among other tested carbonate bases and KO*t*Bu. These strong bases were expected to facilitate enolate formation.^{10b} However, weakly basic acetates were found to be far more effective for this transformation, possibly due to the easily enolizable nature of benzoin. Using CsOAc, 3e was obtained in 75% yield along with a non-PPD structural isomer 4e (13%, entry 2).¹³ The best yield for 3e was achieved by employing KOAc; the combined yield of 3e and 4e reached 95%, and the ratio was 87/13 (entry 3). Although the selectivity was improved with NaOAc, the total yield dropped to 49% (entry 4). The choice of ligand was also crucial. Other bidentate phosphines DPEphos, dppf, and *rac*-BINAP were not as effective as Xantphos was; the total yields decreased to 65%, 52%, and 20%, respectively (entries 5–7). The selectivity (isomer ratio) was much affected, even reversed in the case of dppf and *rac*-BINAP, implying that the catalyst is involved in the selectivity-determining step (see SI for further discussion). As for a catalyst precursor, a divalent palladium source, PdCl₂(PhCN)₂ complex, led to a slight decrease in the yield while maintaining the selectivity, suggesting that the palladium complexes enter the catalytic cycle as Pd(0) species (entry 7). The yield was restored by increasing the amount of KOAc to 3 equiv (entry 8).

With the optimized conditions in hand, we completed the synthesis of fused PPDs by the double carbonylative cyclization of benzoin 2a–2e (Table 2). The conditions were demonstrated to be effective not only for thiophene-derived benzoin but also for benzene-derived benzoin. For example, 2a was

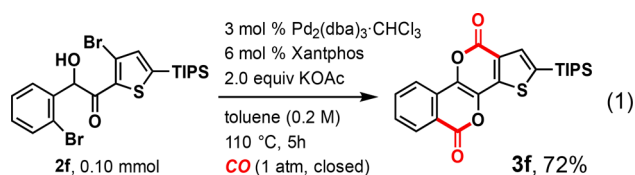
Table 2. Synthesis of Fused PPDs 3a–3e from Benzoin 2a–2e^a

entry	benzoin 2	fused PPD 3	isolated yield 3 (%) 4 (%)	
1			81	6
2			64 ^b	8 ^b
3			66	13
4 ^c			65	6
5			25	—
6			72	6

^aConditions: 2 (0.20 or 0.10 mmol), Pd₂(dba)₃·CHCl₃ (3 mol %), Xantphos (6 mol %), KOAc (2.0 equiv) in toluene (0.2 M) under CO (1 atm, closed) at 110 °C. ^bOn 1.0 mmol scale. ^cAt 90 °C. Si = triisopropylsilyl.

efficiently converted to 3a and 4a in a ratio of 90/10 as judged from ¹H NMR of the crude mixture. Product 3a was isolated in 81% yield after silica-gel column chromatography (entry 1). The same reaction was also performed in 1.0 mmol scale, affording 170 mg of 3a (entry 2). The syntheses of fused PPDs 3b, 3c, and 3e having alkyl chain, fluorine, and silyl substituents, respectively, were also examined because these substituents are often utilized to control crystal packing.^{1a,b,f,14} As a result, those fused PPDs were successfully synthesized and isolated in good yields (65–72%). Thieno-fused PPD without any substituents (3d) was obtained, albeit in low yield, partly owing to its limited solubility.

We further extended the strategy to the synthesis of unsymmetrically fused PPDs. Benzoin 2f was prepared by cyanosilylation of 1a followed by deprotonation with lithium diisopropylamide and trapping with 1e (see Supporting Information (SI) for detail). Double carbonylative cyclization of 2f proceeded efficiently under the standard conditions, affording *benzo-thieno*-fused PPD 3f in 72% isolated yield (eq 1).



All the structures of fused PPDs **3a**–**3f** were unambiguously determined by single-crystal X-ray structure analysis (Figure 2)

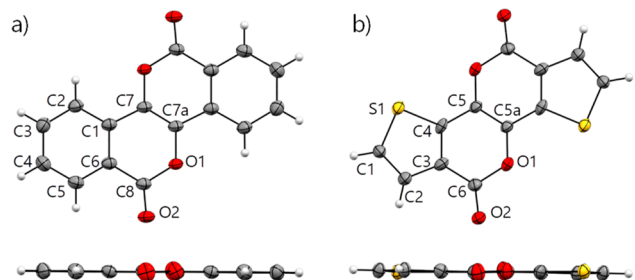


Figure 2. ORTEP drawing of the crystal structures for **3a** (a) and **3d** (b). Thermal ellipsoids are set at the 50% probability level. Selected bond lengths for **3a**: C1–C7, 1.437(2); C7–C7a, 1.341(2) Å. For **3d**: C4–C5, 1.435(7); C5–C5a, 1.343(6) Å.

for **3a** and **3d**; see SI for others). Except **3f** whose skeleton was slightly bent in the crystal, all the other fused PPDs had planar skeletons. All, except **3e**, were packed very tightly (interplanar distances of the parallel stacked pairs: 3.17–3.39 Å) with various short contacts including hydrogen bonding on the carbonyl oxygen. Moreover, their packing modes can be tuned by substituents and the skeleton: herringbone stacking for **3a** and **3c**, brick wall 2D stacking for **3b**, 1D columnar stacking for **3d**, and antiparallel pairwise 1D stacking for **3f**. We also performed thermogravimetric analysis of **3a** and **3d**, which did not show any indication of decomposition (Figure S1). Temperatures for 5% weight loss were at 275 and 317 °C, respectively, both of which corresponding to sublimation of the compounds. As for the electrochemical property, cyclic voltammograms of **3b** and **3e** in tetrahydrofuran were measured. They showed two reversible reduction peaks at –2.71 and –2.31 V for **3b** and –2.37 and –1.91 V for **3e** (versus Fc/Fc⁺), which demonstrated their electrochemical stability and low lying LUMO (–2.5 eV for **3b** and –2.9 eV for **3e**, Figures S2 and S3).^{5,6} These thermal and electrical properties as well as tunable molecular arrangements in crystal indicate that fused PPDs are promising materials for the application in organic electronics.

UV–vis absorption and photoluminescence (PL) spectra as well as photoluminescence quantum yields (Φ_F)¹⁵ of fused PPDs were measured in degassed dichloromethane (Figure 3 and Table 3 for representative data; see SI for full details). For all fused PPDs **3a**–**3f**, UV–vis and PL spectra are mirror images of each other with vibrational structure, and the Stokes shifts are very small. These features imply their rigidity and structural similarity in the ground state (S₀) and the first singlet excited state (S₁). More specifically, along with replacing the peripheral fused ring from benzene to thiophene (i.e., **3a** → **3f** → **3e**, from bottom to top in Figure 3), the vibrational structure became sharper with progression of 0–0 band, and the Stokes shifts became smaller (11 nm for **3a**, 9 nm for **3f**, and 4 nm for **3e**). These trends clearly indicate that the structural displacement in S₁ becomes much smaller in this order. In addition, both UV–vis and PL spectra are bathochromically shifted about 40 nm in

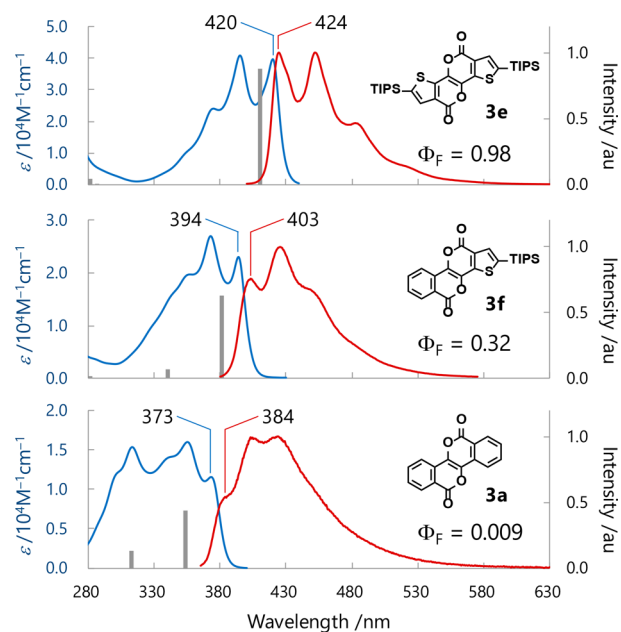


Figure 3. UV–vis absorption (blue) and normalized PL (red) spectra for **3e** (top), **3f** (middle), and **3a** (bottom) in CH₂Cl₂. Oscillator strengths of absorption (TD-DFT//B3LYP/6-31+G**) are depicted as gray bars. Φ_F are relative to quinine sulfate.¹⁵ Left axis for UV–vis, right axis for others.

Table 3. Photophysical Properties of 3a–3f and 4e

compd	λ_{abs} (nm) ^a	ϵ (M ⁻¹ cm ⁻¹) ^b	λ_{em} (nm) ^c	Φ_F ^d	k_r (ns ⁻¹) ^e	k_{nr} (ns ⁻¹) ^e
3a	373	16 000	384	0.009	0.29 ^f	32 ^f
3b	382	19 600	395	0.049	n.d.	n.d.
3c	364	18 100	370	0.004	n.d.	n.d.
3f	394	26 900	403	0.32	0.37	0.79
3d	408	33 700	413	0.90	0.38	0.042
3e	420	40 800	424	0.98	0.38	0.0078
4e	419	45 900	427	0.31	0.41	0.92

^aThe longest absorption maxima. ^bAt the global maxima. ^cThe shortest emission maxima. ^dDetermined relative to quinine sulfate.¹⁵ ^eCalculated with Φ_F and τ according to the formula $k_r = \Phi_F/\tau$ and $k_{\text{nr}} = (1 - \Phi_F)/\tau$. ^fCalculated with λ_{em} , oscillator strength, and Φ_F . See Table S2 in SI for detail. n.d. = not determined.

total, suggesting that thieno-fused systems have a smaller HOMO–LUMO gap and more delocalized π -system than benzo-fused ones do. Indeed, according to time-dependent density functional theory (TD-DFT) calculation at the B3LYP/6-31+G(d,p) level of theory, the strongest transitions in **3a**, **3f**, and **3e** are of S₀–S₁ (HOMO–LUMO 94% or more) and are essentially a π – π^* transition in nature, for both absorption and emission.

The peripheral aromatic rings most substantially effected Φ_F . Thieno-fused PPDs **3d** and **3e** exhibited much higher Φ_F (≥ 0.9) than benzo-fused PPDs **3a**–**3c** did ($\Phi_F < 0.1$). The highest Φ_F was observed for **3e** (0.98) while **3d** still showed a high Φ_F of 0.90, suggesting that the highly fluorescent nature is attributed to the core skeleton itself, rather than to the silyl substituent.¹⁶ This is also evident from a comparison of **3e** and its structural isomer **4e**. Their UV/PL spectra were similar in peak positions and molar extinction coefficient (ϵ); however, **4e** showed somewhat broadened spectra (Figure S4), as well as a much diminished quantum yield of 0.31. This emphasizes the

superiority of the PPD core for the structural rigidity even in the excited states.

We further evaluated the radiative and nonradiative decay rate constants (k_r and k_{nr}) of **3a**, **3d–3f**, and **4e** (Table 3; see SI for details). According to the equation $\Phi_F = k_r / (k_r + k_{nr})$, it is clearly revealed that the strong dependency of Φ_F on their fused aromatics originates from a difference in k_{nr} , which is 4 orders of magnitude for **3a** to **3e**. In addition, **4e** exhibits a 2-order larger k_{nr} than that of **3e**. These trends in the rate constants again prove the structural rigidity, or more specifically, the sharpness of potential energy surface¹⁷ of fused PPDs especially for thieno-fused ones. It should be noted that k_{nr} includes intersystem crossing. Nonetheless, a negligible decrease of PL intensity was observed under air-saturated condition. Moreover, the PL spectrum of **3a** measured at 77 K in 2-methyltetrahydrofuran displayed imperceptible phosphorescence (Figure S6). Thus, the intersystem crossing is sufficiently slower than the radiative S1–S0 decay and can be ignored in the photophysical process.

In summary, we have developed a novel Pd-catalyzed double carbonylative cyclization of benzoin, and established the versatile synthesis of bis-ester-bridged stilbenes in two steps from aldehydes. They exhibited unique thermal and electrical properties as well as tunable crystal packing, owing to the carbonyl functionality. Moreover, their photophysical properties unexpectedly depend on the peripheral aromatic rings fused to the PPD core, and bis-thieno-fused PPDs are demonstrated to be a novel class of excellent fluorophores. Further studies to exploit the potential of the fused PPDs are ongoing in our laboratory.

■ ASSOCIATED CONTENT

■ Supporting Information

The Supporting Information is available free of charge on the ACS Publications website at DOI: 10.1021/acs.orglett.8b03169.

Experimental procedures, characterization of new compounds, physicochemical properties, and theoretical calculations (PDF)

Accession Codes

CCDC 1858128–1858129 and 1859329–1859333 contain the supplementary crystallographic data for this paper. These data can be obtained free of charge via www.ccdc.cam.ac.uk/data_request/cif, or by emailing data_request@ccdc.cam.ac.uk, or by contacting The Cambridge Crystallographic Data Centre, 12 Union Road, Cambridge CB2 1EZ, UK; fax: +44 1223 336033.

■ AUTHOR INFORMATION

Corresponding Authors

*E-mail: y-tani@chem.sci.osaka-u.ac.jp.

*E-mail: ogawa@chem.sci.osaka-u.ac.jp.

ORCID

Yosuke Tani: 0000-0003-1326-5457

Notes

The authors declare no competing financial interest.

■ ACKNOWLEDGMENTS

This work was supported by the JSPS KAKENHI (Grant Numbers JP25110002 and JP17K17863). Y.T. is grateful to the Kyoto Technoscience Center for the financial support. We deeply thank Dr. Soichiro Kawamori and Prof. Dr. Takeshi

Naota (Osaka University) for their assistance with the lifetime and low-temperature photoluminescence measurement. The theoretical calculations were partly performed using the Research Center for Computational Science, Okazaki, Japan.

■ REFERENCES

- (1) For reviews focusing on the optical and electronic properties of polycyclic fused π -systems, see: (a) Takimiya, K.; Osaka, I.; Mori, T.; Nakano, M. Organic Semiconductors Based on [1]Benzothieno[3,2-*b*][1]benzothiophene Substructure. *Acc. Chem. Res.* **2014**, *47*, 1493–1502. (b) Takimiya, K.; Shinamura, S.; Osaka, I.; Miyazaki, E. Thienoacene-Based Organic Semiconductors. *Adv. Mater.* **2011**, *23*, 4347–4370. (c) Sergeev, S.; Pisula, W.; Geerts, Y. H. Discotic liquid crystals: a new generation of organic semiconductors. *Chem. Soc. Rev.* **2007**, *36*, 1902–1929. (d) Laschat, S.; Baro, A.; Steinke, N.; Giesselmann, F.; Hägele, C.; Scalia, G.; Judele, R.; Kapatsina, E.; Sauer, S.; Schreivogel, A.; Tosoni, M. Discotic Liquid Crystals: From Tailor-Made Synthesis to Plastic Electronics. *Angew. Chem., Int. Ed.* **2007**, *46*, 4832–4887. (e) Grimsdale, A. C.; Müllen, K. Oligomers and Polymers Based on Bridged Phenyls as Electronic Materials. *Macromol. Rapid Commun.* **2007**, *28*, 1676–1702. (f) Anthony, J. E. Functionalized Acenes and Heteroacenes for Organic Electronics. *Chem. Rev.* **2006**, *106*, 5028–5048. For recent examples on application of bridged stilbenes, see: (g) Ryoo, C. H.; Cho, I.; Han, J.; Yang, J.-h.; Kwon, J. E.; Kim, S.; Jeong, H.; Lee, C.; Park, S. Y. Structure–Property Correlation in Luminescent Indolo[3,2-*b*]indole (IDID) Derivatives: Unraveling the Mechanism of High Efficiency Thermally Activated Delayed Fluorescence (TADF). *ACS Appl. Mater. Interfaces* **2017**, *9*, 41413–41420. (h) Nishioka, H.; Tsuji, H.; Nakamura, E. Homo- and Copolymers Based on Carbon-Bridged Oligo(*p*-phenylenevinylene)s for Efficient Fluorescence over the Entire Visible Region. *Macromolecules* **2018**, *51*, 2961–2968.
- (2) For recently emerging synthetic approaches, see: (a) Koga, Y.; Kaneda, T.; Saito, Y.; Murakami, K.; Itami, K. Synthesis of partially and fully fused polyaromatics by annulative chlorophenylene dimerization. *Science* **2018**, *359*, 435–439. (b) Oshima, H.; Fukazawa, A.; Yamaguchi, S. Facile Synthesis of Polycyclic Pentalenes with Enhanced Hückel Antiaromaticity. *Angew. Chem., Int. Ed.* **2017**, *56*, 3270–3274. (c) Ito, H.; Ozaki, K.; Itami, K. Annulative π -Extension (APEX): Rapid Access to Fused Arenes, Heteroarenes, and Nanographenes. *Angew. Chem., Int. Ed.* **2017**, *56*, 11144–11164. (d) Shintani, R.; Iino, R.; Nozaki, K. Rhodium-Catalyzed Stitching Reaction: Convergent Synthesis of Quinoidal Fused Oligosiloles. *J. Am. Chem. Soc.* **2016**, *138*, 3635–3638. (e) Maekawa, T.; Segawa, Y.; Itami, K. C–H activation route to dibenzo[*a,e*]pentalenes: annulation of arylacetylenes promoted by PdCl₂–AgOTf–*o*-chloranil. *Chem. Sci.* **2013**, *4*, 2369–2373.
- (3) (a) Kurata, Y.; Otsuka, S.; Fukui, N.; Nogi, K.; Yorimitsu, H.; Osuka, A. Aromatic Metamorphosis of Dibenzofurans into Triphenylenes Starting with Nickel-Catalyzed Ring-Opening C–O Arylation. *Org. Lett.* **2017**, *19*, 1274–1277. (b) Narita, A.; Wang, X.-Y.; Feng, X.; Müllen, K. New advances in nanographene chemistry. *Chem. Soc. Rev.* **2015**, *44*, 6616–6643. (c) Mori, T.; Nishimura, T.; Yamamoto, T.; Doi, I.; Miyazaki, E.; Osaka, I.; Takimiya, K. Consecutive Thiophene-Annulation Approach to π -Extended Thienoacene-Based Organic Semiconductors with [1]Benzothieno[3,2-*b*][1]benzothiophene (BTBT) Substructure. *J. Am. Chem. Soc.* **2013**, *135*, 13900–13913. (d) Kawasumi, K.; Zhang, Q.; Segawa, Y.; Scott, L. T.; Itami, K. A grossly warped nanographene and the consequences of multiple odd-membered-ring defects. *Nat. Chem.* **2013**, *5*, 739–744. (e) Grzybowski, M.; Skonieczny, K.; Butenschön, H.; Gryko, D. T. Comparison of Oxidative Aromatic Coupling and the Scholl Reaction. *Angew. Chem., Int. Ed.* **2013**, *52*, 9900–9930. (f) Mochida, K.; Shimizu, M.; Hiyama, T. Palladium-Catalyzed Intramolecular Coupling of 2-[(2-pyrrolyl)silyl]aryl Triflates through 1,2-Silicon Migration. *J. Am. Chem. Soc.* **2009**, *131*, 8350–8351.
- (4) (a) Cai, J.; Wu, B.; Rong, G.; Zhang, C.; Qiu, L.; Xu, X. Gold-catalyzed Bicyclization of Diaryl Alkynes: Synthesis of Polycyclic Fused

- Indole and Spirooxindole Derivatives. *Org. Lett.* **2018**, *20*, 2733–2736.
- (b) Yu, J.; Zhang-Negrerie, D.; Du, Y. Cu(OAc)₂-Mediated Cascade Annulation of Diarylalkyne Sulfonamides through Dual C–N Bond Formation: Synthesis of 5,10-Dihydroindolo[3,2-*b*]indoles. *Org. Lett.* **2016**, *18*, 3322–3325. (c) Matsumura, M.; Muranaka, A.; Kurihara, R.; Kanai, M.; Yoshida, K.; Kakusawa, N.; Hashizume, D.; Uchiyama, M.; Yasuike, S. General synthesis, structure, and optical properties of benzothiophene-fused benzoheteroles containing Group 15 and 16 elements. *Tetrahedron* **2016**, *72*, 8085–8090. (d) Ho, H. E.; Oniwa, K.; Yamamoto, Y.; Jin, T. *N*-Methyl Transfer Induced Copper-Mediated Oxidative Diamination of Alkynes. *Org. Lett.* **2016**, *18*, 2487–2490. (e) Zhang, Q.-W.; An, K.; He, W. Rhodium-Catalyzed Tandem Cyclization/Si–C Activation Reaction for the Synthesis of Siloles. *Angew. Chem., Int. Ed.* **2014**, *53*, 5667–5671. (f) Dou, C.; Saito, S.; Gao, L.; Matsumoto, N.; Karasawa, T.; Zhang, H.; Fukazawa, A.; Yamaguchi, S. Sequential Electrophilic and Photochemical Cyclizations from Bis(bithienyl)acetylene to a Tetrathienonaphthalene Core. *Org. Lett.* **2013**, *15*, 80–83. (g) Araneda, J. F.; Neue, B.; Piers, W. E.; Parvez, M. Photochemical Synthesis of a Ladder Diborole: A New Boron-Containing Conjugate Material. *Angew. Chem., Int. Ed.* **2012**, *51*, 8546–8550. (h) Iida, A.; Yamaguchi, S. Thiophene-Fused Ladder Boroles with High Antiaromaticity. *J. Am. Chem. Soc.* **2011**, *133*, 6952–6955. (i) Zhu, X.; Mitsui, C.; Tsuji, H.; Nakamura, E. Modular synthesis of 1*H*-indenes, dihydro-*s*-indacene, and diindenoindacene—a carbon-bridged *p*-phenylenevinylene congener. *J. Am. Chem. Soc.* **2009**, *131*, 13596–13597. (j) Fukazawa, A.; Yamaguchi, S. Ladder π -Conjugated Materials Containing Main-Group Elements. *Chem. - Asian J.* **2009**, *4*, 1386–1400. (k) Fukazawa, A.; Hara, M.; Okamoto, T.; Son, E. C.; Xu, C.; Tamao, K.; Yamaguchi, S. Bis-phosphoryl-bridged stilbenes synthesized by an intramolecular cascade cyclization. *Org. Lett.* **2008**, *10*, 913–916. (l) Takimiya, K.; Kunugi, Y.; Konda, Y.; Ebata, H.; Toyoshima, Y.; Otsubo, T. 2,7-Diphenyl[1]benzoselenopheno[3,2-*b*] [1]benzoselenophene as a Stable Organic Semiconductor for a High-Performance Field-Effect Transistor. *J. Am. Chem. Soc.* **2006**, *128*, 3044–3050.
- (5) Shinamura, S.; Miyazaki, E.; Takimiya, K. Synthesis, Properties, Crystal Structures, and Semiconductor Characteristics of Naphtho[1,2-*b*:5,6-*b'*]dithiophene and -diselenophene Derivatives. *J. Org. Chem.* **2010**, *75*, 1228–1234.
- (6) According to the molecular orbital calculations, LUMO levels of bis-ester-bridged stilbenes are substantially lower than that of chrysene or a methylene-bridged stilbene, and comparable to that of phosphoryl-bridged stilbene (Figure S3 in SI). See also refs 4k and 5.
- (7) (a) Cheng, F.; Deng, Z.; Guo, Z.; Chen, J.; Zou, K. Machilusmarin, a new neuroprotective isocoumarin dimer from the stems of *Machilus ichangensis* Rehd. et Wils. *Nat. Prod. Res.* **2013**, *27*, 1542–1547. (b) Snyder, J.; Nakanishi, K.; Chaverria, G.; Leal, Y.; Ochoa, C. C.; Dominguez, X. A. The structure of castanaguyone a bisocoumarin plant product. *Tetrahedron Lett.* **1981**, *22*, 5015–5018.
- (8) Bis-ester-bridged stilbene has been obtained as a major product from benzocyclobutene-1,2-dione^{8f} or **4a** (see Table 2 for general structure).^{8c} To our knowledge, none of the thieno-fused analogs have been synthesized. (a) Cava, M. P.; Napier, D. R.; Pohl, R. J. Condensed Cyclobutane Aromatic Compounds. XXVI. Benzocyclobutadienoquinone: Synthesis and Simple Transformations. *J. Am. Chem. Soc.* **1963**, *85*, 2076–2080. (b) Bisagni, E.; Marquet, J. P.; Jeannine, A.-L. Furans and Pyrroles Disubstituted in 2 and 3 Positions. 2. Synthesis of 2-Formyl-3-Carboethoxy Furans and Pyrroles and their Transformations by means of Potassium Cyanide. *Bull. Soc. Chim. Fr.* **1968**, 637–645. (c) Bird, C. W.; Wong, D. Y. Organophosphorus Intermediates—II. Deoxygenative Dimerisation of Maleic Anhydrides by Triethyl Phosphite. *Tetrahedron* **1975**, *31*, 31–32. (d) Ramirez, F.; Ricci, J. S.; Tsuboi, H.; Marecek, J. F.; Yamanaka, H. Crystal and molecular structure of trans-biphthalyl, C₁₆H₈O₄. Reaction of substituted phthalic anhydrides with trialkyl phosphites. *J. Org. Chem.* **1976**, *41*, 3909–3914. (e) Kaupp, G.; Schmitt, D. Dispirocyclobutane und Propellane aus 1,2-Bisenollactonen. *Chem. Ber.* **1981**, *114*, 1983–1990. (f) Buckland, P. R.; Hacker, N. P.; McOmie, J. F. W. Biphenylenes. Part 32. A new, general synthesis of mono- and poly-benzobiphenylenes from substituted benzocyclobutene-1,2-diones and ortho-bis(cyanomethyl)-arenes. *J. Chem. Soc., Perkin Trans. 1* **1983**, 1443–1448.
- (9) (a) Brennfürer, A.; Neumann, H.; Beller, M. Palladium-Catalyzed Carbonylation Reactions of Aryl Halides and Related Compounds. *Angew. Chem., Int. Ed.* **2009**, *48*, 4114–4133. (b) Martinelli, J. R.; Watson, D. A.; Freckmann, D. M. M.; Barder, T. E.; Buchwald, S. L. Palladium-Catalyzed Carbonylation Reactions of Aryl Bromides at Atmospheric Pressure: A General System Based on Xantphos. *J. Org. Chem.* **2008**, *73*, 7102–7107.
- (10) (a) Wu, X.-F.; Neumann, H.; Beller, M. Synthesis of Heterocycles via Palladium-Catalyzed Carbonylations. *Chem. Rev.* **2013**, *113*, 1–35. (b) Tadd, A. C.; Fielding, M. R.; Willis, M. C. Palladium-catalyzed aryl halide carbonylation—intramolecular O-enolate acylation: efficient isocoumarin synthesis, including the synthesis of thunberginol A. *Chem. Commun.* **2009**, 6744–6746.
- (11) Zeng, F.; Alper, H. One-Step Synthesis of Quinazolino[3,2-*a*]quinazolinones via Palladium-Catalyzed Domino Addition/Carboxamidation Reactions. *Org. Lett.* **2010**, *12*, 3642–3644.
- (12) (a) Liu, X.-H.; Park, H.; Hu, J.-H.; Hu, Y.; Zhang, Q.-L.; Wang, B.-L.; Sun, B.; Yeung, K.-S.; Zhang, F.-L.; Yu, J.-Q. Diverse ortho-C(sp²)-H Functionalization of Benzaldehydes Using Transient Directing Groups. *J. Am. Chem. Soc.* **2017**, *139*, 888–896. (b) Comins, D. L.; Brown, J. D. Ortho metalation directed by α -amino alkoxides. *J. Org. Chem.* **1984**, *49*, 1078–1083. (c) Schnürch, M.; Spina, M.; Khan, A. F.; Mihovilovic, M. D.; Stanetty, P. Halogen dance reactions—A review. *Chem. Soc. Rev.* **2007**, *36*, 1046–1057.
- (13) Triethylamine was also ineffective as a base.
- (14) (a) Cho, I.; Jeon, N. J.; Kwon, O. K.; Kim, D. W.; Jung, E. H.; Noh, J. H.; Seo, J.; Seok, S. I.; Park, S. Y. Indolo[3,2-*b*]indole-based crystalline hole-transporting material for highly efficient perovskite solar cells. *Chem. Sci.* **2017**, *8*, 734–741. (b) Dou, J.-H.; Zheng, Y.-Q.; Yao, Z.-F.; Yu, Z.-A.; Lei, T.; Shen, X.; Luo, X.-Y.; Sun, J.; Zhang, S.-D.; Ding, Y.-F.; Han, G.; Yi, Y.; Wang, J.-Y.; Pei, J. Fine-Tuning of Crystal Packing and Charge Transport Properties of BDOPV Derivatives through Fluorine Substitution. *J. Am. Chem. Soc.* **2015**, *137*, 15947–15956.
- (15) (a) Brouwer, A. M. Standards for photoluminescence quantum yield measurements in solution (IUPAC Technical Report). *Pure Appl. Chem.* **2011**, *83*, 2213–2228. (b) Suzuki, K.; Kobayashi, A.; Kaneko, S.; Takehira, K.; Yoshihara, T.; Ishida, H.; Shiina, Y.; Oishi, S.; Tobita, S. Reevaluation of absolute luminescence quantum yields of standard solutions using a spectrometer with an integrating sphere and a back-thinned CCD detector. *Phys. Chem. Chem. Phys.* **2009**, *11*, 9850–9860.
- (16) According to DFT calculation for **3e**, σ -bonds of silicon and methine carbon of isopropyl group participate in its HOMO, which may account for the higher Φ_F of **3e** than **3d** (Figure S12). See also: Shimizu, M.; Shigitani, R.; Nakatani, M.; Kuwabara, K.; Miyake, Y.; Tajima, K.; Sakai, H.; Hasobe, T. Siloxy Group-Induced Highly Efficient Room Temperature Phosphorescence with Long Lifetime. *J. Phys. Chem. C* **2016**, *120*, 11631–11639.
- (17) Tokieda, D.; Tsukamoto, T.; Ishida, Y.; Ichihara, H.; Shimada, T.; Takagi, S. Unique fluorescence behavior of dyes on the clay minerals surface: Surface Fixation Induced Emission (S-FIE). *J. Photochem. Photobiol., A* **2017**, *339*, 67–79.